Response to Referees' Comments

Response to Reviewer #2:

The manuscript addresses a critical and challenging issue in aerosol effects on weather and climate, i.e. the influence of aerosol vertical structure on boundary layer stability and height. The two-year concurrent observations from micropulse lidar, sun-photometer, and radiosonde were employed to provide direct and quantitative evidence on the aerosol radiative effects on the boundary layer development. The contrasting effects of different aerosol vertical structures identified by this study are important to know and call on a better representation of aerosol vertical profile in numerical models for future aerosol effect assessment. The paper is well written overall, and its scientific merit is clear. I recommend its publication with ACP, while I also have comments below for the authors to address.

Response: We appreciate the reviewer's positive and constructive comments on our work. All of the comments and concerns raised by the referee have been carefully considered and incorporated into this revision. Our detailed responses to the reviewer's questions and comments are listed below.

1. *Figure 2, are the data here from three cases or composites from all available observations? I have the similar question for Figs. 3-7 as well. Please clarify the data source and sampling range in the figure captions.*

Response: We clarify that the results are averaged from all available observations during the study period. We added the number of samples in the panels or in the descriptions of the figures. The latter are carefully checked to assure that the data sources are clearly stated.

2. *Is R* in Figure 3 for linear regression and R* in Figure 5 for the inverse fitting?*

Better to use different symbols for different types of regression.

Response: Revised, per your suggestion.

3. *As shown in Figure 5, the weakly absorbing aerosols can also suppress PBLH. I assume it is caused by the reduction in solar radiation reaching the surface and the consequent suppression in surface latent/sensible heat fluxes. Since the authors have performed the radiation transfer simulations, I'm wondering if they can illustrate the importance of atmospheric heating and surface cooling for PBL development when absorbing aerosols are present.*

Response: Thanks for raising this point. We clarify that both absorbing and weakly absorbing aerosols reduce the radiation reaching the lower atmosphere and the surface, thus suppressing the PBLH. Both decreasing and inverse aerosol structures can cool the surface and suppress sensible heat, thereby stabilizing the PBL. Despite the different aerosol structures, aerosols cause a notable stabilizing effect near the surface.

On the other hand, for the decreasing with height structure, the abundance of aerosols near the surface generates a stronger aerosol heating rate in the lower PBL than in the upper PBL. Such aerosol radiative forcing decreases the potential temperature gradient ($d\theta/dz$) in the middle to upper PBL, further strengthening vertical convection in the middle to upper PBL. The opposite aerosol effects on PBL stability weakens the aerosol-PBL feedback, as is shown in our study. For the inverse aerosol structure, the significant heating effect in the upper PBL facilitates the formation of a temperature inversion and further increases the stability and suppresses the PBLH. The notable increase in stability lead to the strong, positive aerosol feedback, as is demonstrated in Figure R1 (the revised Figure 9).

Turbulent fluxes and eddies in the PBL can spread out and redistribute the radiative effects induced by aerosols. We need to resort to numerical simulations to quantify the aerosol impacts on the PBL. Since the aerosol vertical distribution

is still poorly represented in numerical models, improvements in model simulations are warranted to better understand the aerosol-PBL interaction quantitatively. This is an ongoing study by our team that will be presented in a future paper.

A detailed discussion has been incorporated into the revised Section 3.3 and Section 4.

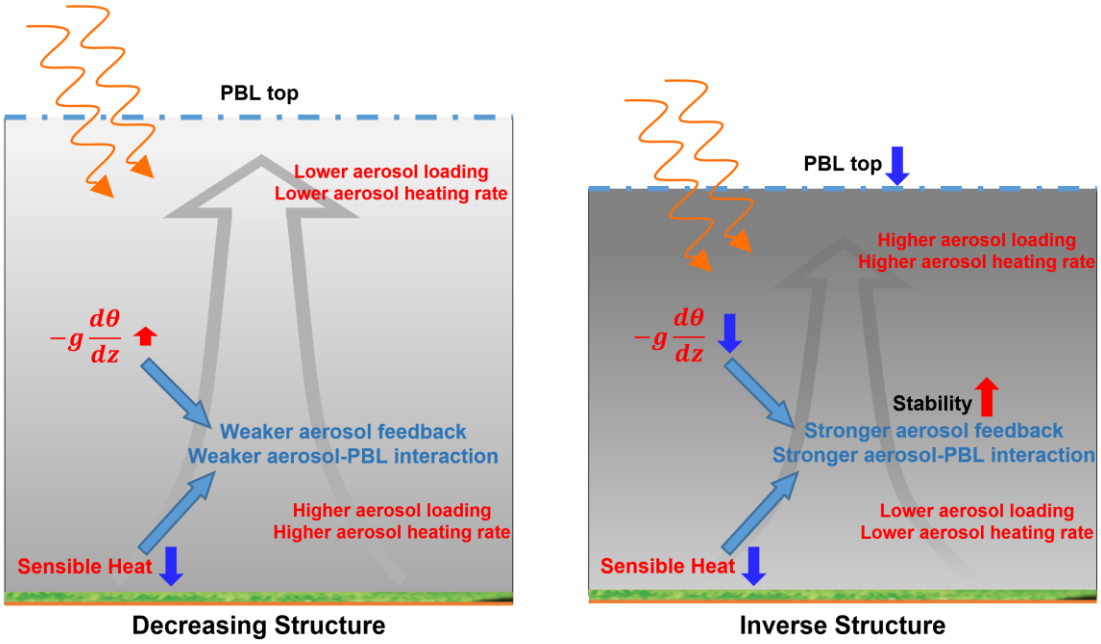

Figure R1. Schematic diagrams describing aerosol-PBL interactions when decreasing and inverse aerosol structures are present. The blue dash-dotted line indicates the top of the PBL. Orange curved arrows indicate solar radiation. The background grey arrow shows the vertical transport of humidity, aerosols, and heat. The background greyscale indicates the pollution level.

4. *L285-286, the sentence is hard to follow. What do you mean by "significant heating in the different parts of PBL"?*

Response: We revised this sentence as follows:

"Figure 7 shows that the vertical distributions of the heating rate differ drastically

among the different aerosol structures."

5. *Since the authors possess ample observations data, can you show the occurrence/frequency of each aerosol vertical structure within PBL (decreasing, inverse, and well-mixed)? It is interesting to know the relative importance of those three structures in the real atmosphere. Moreover, can you sort out what factors determine those distributions within PBL?*

Response: Per your guidance, we present the number of samples for each aerosol structure during the study period in the revised Section 3.1.

"The number of samples and percentages of decreasing, well-mixed, and increasing aerosol structures are 998 (51%), 611 (32%), and 330 (17%), respectively."

The decreasing structure is more frequent during the afternoon, partly due to the entrainment process. Through the development of a PBL, entrainment brings dry and clean air from the free atmosphere into the PBL, diluting the aerosol loading in the upper PBL. Note that multiple entangled factors can contribute to the formation of different aerosol structures within the PBL, including synoptic patterns, new particle formation, vertical turbulence, horizontal transport, entrainment rates, to name a few. The complexity of this issue is an important reason for the poor representation of the aerosol vertical distribution in numerical models.

This discussion has been incorporated into the revised Section 3.2.

6. *L309-315 and Figure 9. What is the physical/chemical mechanism of the negative feedback, i.e. stable PBL leads to less aerosol formation? The color of big red arrow in the upper part of Figure should be changed to blue, as it is about negative feedback.*

Response: A low PBLH and high stability increase the aerosol loading. This mechanism is straightforward and clear. We investigate the opposite effect: how aerosols affect the PBL via their feedbacks. If the aerosol heating effect is much stronger on near surface than upper PBL, aerosol can decrease the stability in PBL, and cause the negative feedback. Negative feedback partly offset the PBL's impact on the aerosol loading. The large variations in the impact of aerosols on stability and PBL development lead to different magnitudes in the aerosol-PBL interaction.

This discussion has been incorporated into the revised Section 3.3. We also use a revised figure (Figure R1) to replace the previous Figure 9 to better demonstrate the interactions.

7. *L334, it should be Wang et al. 2013.*

Response: Revised.

8. *Please remove "conclusive" from the title, as it is a very subjective word.*

Response: Per your comment, we changed it to "significant".

Response to Reviewer #1:

Aerosol-planetary boundary layer (PBL) interaction is proposed as an important mechanism to stabilize the atmosphere and exacerbate surface air pollution. Attempts to analyze aerosol-PBL interaction by using observation data are rare and worth encouraging. Thus, I recommend a minor revision before publication. The detail comments or suggestions are shown below:

Response: We appreciate the reviewer's positive and constructive comments on our work. All of the comments and concerns raised by the referee have been carefully considered and incorporated into this revision. Our detailed responses to the reviewer's questions and comments are listed below.

1. *My main concern about this study is how to get cause-effect from correlations. As we know, PBL has a strong impact on surface aerosol concentration and aerosol vertical profile (forward effect). Compared to that, the impact of aerosol on PBL (reverse effect) can be treated as a perturbation. Thus, it is hard to get the contribution of reverse effect only. For example, Line 265 to 272. It is claimed that "In general, there are stronger correlations between PBLH and PM2.5 under inverse aerosols structure. This phenomenon indicates that the absorbing aerosol could play a more important role in the inverse aerosol structure.". Let's imagine that the decreasing and inverse profile are formed by specific PBL structure, we may get a similar relationship between PBL height and PM2.5 in Figure 5. Moreover, it is possible that the correlations are caused by some other factors, simultaneously, like the front process or precipitation.*

Response: Indeed, the PBL and aerosols mutually affect each other. While it is challenging to differentiate their respective impacts on each other, we have used the MPL-derived PBLH and in situ $PM_{2.5}$ data to show their correlation, which can indicate the overall intensity of aerosol-PBL interaction, but cannot represent the feedback intensity. Since we considered only cloud-free cases, rainfall would

not affect the correlations. But many other factors do affect the PBLH- $PM_{2.5}$ correlations, as well as the aerosol-PBL interaction. Therefore, the correlations cannot explain the causality and aerosol feedback loop. The correlations between PBLH and $PM_{2.5}$ provide hints about the differences in aerosol-PBL interactions for different aerosol structures. Using SBDART constrained by ample observations, we investigated the vertical profiles of radiative forcing induced by aerosols and its impacts on atmospheric stability.

A detailed discussion has been incorporated into the revised Section 3.2.

2. *I don't quite understand the role of Figure 6 and the corresponding part of the manuscript. It seems that Figure 6 does not support the topic directly and may be considered to be moved to SI.*

Response: We apologize for not clearly describing and elaborating on the role of Figure 6 in making an important point.

In general, the inverse structure is characterized by higher aerosol loading and a lower PBLH, whereas the decreasing structure is characterized by light pollution and a well-developed PBL. For the inverse structure, the lower PBLH growth rate, along with high aerosol loading, can be explained by the strong aerosol-PBL interaction. The diurnal variations in aerosols and the PBL are controlled by many factors. The strong aerosol-stability interaction generates an unfavorable condition for aerosol vertical dissipation in the vertical, so surface aerosol loading can continuously accumulate due to emissions.

The discussion has been incorporated into the revised Section 3.2.

3. *More quantitative analysis is needed in the Results part. I can barely find the detail of quantitative discussion figures, especially in 3.3. I'm not sure if Figure 7 is a specific case, a statistic scenario or just a diagram? It seems there are too many*

diagrams in the manuscript.

Response: Figure 7 presents statistical results derived from all available measurements (same as Figure 6). We revised the figure description to avoid any misunderstanding. Based on observations, we calculate the aerosol radiative forcing by SBDART for all cases. We can then obtain averaged diurnal cycles of the vertical profile of aerosol radiative forcing for different aerosol structures.

4. *It might be helpful to show some statistical information and meteorological condition information. For example, the occurrence/frequency of each aerosol vertical structure within PBL. Does it occur in specific seasons or weather conditions?*

Response: We added the number of AEC profiles for different aerosol structures during the study period in the revised Section 3.1.

"The number of samples and percentages of decreasing, well-mixed, and increasing aerosol structures are 998 (51%), 611 (32%), and 330 (17%), respectively."

All three types of profiles commonly occur in the real atmosphere. The decreasing structure is more frequent during the afternoon, partly due to the entrainment at the top of a PBL. Through the PBL development, entrainment brings dry and clean air from the free atmosphere into the PBL, diluting the aerosol loading in the upper PBL.

Multiple entangled factors are related to the formation of different aerosol structures within the PBL, including synoptic patterns, new particle formation, vertical turbulence, horizontal transport, entrainment rates, to name a few. The complexity of this issue is an important reason for the poor representation of aerosol vertical distributions in numerical models. We will further investigate this issue, which will be presented in a future paper.

The ~~conclusive~~significant impact of aerosol vertical structure on lower-atmosphere stability and its critical role in aerosol-PBL interactions

Tianning Su[1], Zhanqing Li[1,2*], Chengcai Li[2], Jing Li[2], Wenchao Han[1,23], Chuanyang Shen[2,4], Wangshu Tan[2], Jing Wei[1,3], Jianping Guo[5]

[1]Department of Atmospheric and Oceanic Sciences & ESSIC, University of Maryland , College Park, Maryland 20740, USA

[2]~~State~~[2]Department of Atmospheric and Oceanic Sciences, Peking University, Beijing 100871, China

[3]State Key Laboratory of ~~Earth Surface Processes and Resource Ecology~~Remote Sensing Science and College of Global Change and Earth System Science, Beijing Normal University, 100875, Beijing, China

~~[3]Department of Atmospheric and Oceanic Sciences, Peking University, Beijing 100871, China~~

[4]Department of Earth, Atmospheric and Planetary Sciences, Massachusetts Institute of Technology, Cambridge, MA, USA

[5]State Key Laboratory of Severe Weather, Chinese Academy of Meteorological Sciences, Beijing 100081, China

∗ Correspondence to: zli@atmos.umd.edu

Formatted: Indent: First line: 0.29"

Formatted: Tab stops: 0.38", Left

Abstract. Aerosol-planetary boundary layer (PBL) interaction was proposed as an important mechanism to stabilize the atmosphere and exacerbate surface air pollution. Despite the tremendous progress made in understanding this process, its magnitude and significance still ~~bear~~have large uncertainties and vary largely with aerosol distribution and meteorological conditions. In this study, we ~~particularly~~ focus on the role of aerosol vertical distribution on thermodynamic stability and PBL development by jointly using ~~the~~ micropulse lidar, ~~sun photometer~~sunphotometer, and radiosonde measurements ~~over~~taken in Beijing. Despite ~~complex~~ the complexity of aerosol vertical distributions, ~~the~~ cloud-free aerosol structures can be largely classified into three types: well-mixed, decreasing with height, and ~~the inversed. Under these different aerosol vertical~~inverse structures~~, the~~. The aerosol-PBL ~~relationships~~relationship and ~~the~~ diurnal cycles of the ~~PBLH~~PBL height and $PM_{2.5}$ associated with these different aerosol vertical structures show distinct ~~characters.~~characteristics. The vertical distribution of aerosol radiative forcing differs drastically among the three types with strong heating in the lower, ~~mid~~middle, and upper PBL, respectively. Such a discrepancy in heating rate affects the atmospheric buoyancy and stability differently in the three distinct aerosol structures. Absorbing ~~aerosol~~aerosols have ~~a~~the weak effect of stabilizing the ~~low~~ lower atmosphere under the decreasing structure than under the inverse structure. As a result, the aerosol-PBL interaction can be strengthened by the inverse aerosol structure, and can be potentially neutralized by the decreasing structure. Moreover, aerosols can both enhance and suppress the PBL stability, leading to both positive and negative feedback loops. This study attempts to improve our understanding of the aerosol-PBL interaction,

~~which shows~~showing the importance of the ~~observation~~observational constraint of aerosol vertical distribution for simulating ~~the~~this interaction and consequent feedbacks.

1. Introduction

Aerosols ~~critically~~have a critical impact on the ~~Earth's~~earth's climate through aerosol-cloud interactions (ACI) and aerosol-radiation interactions (ARI~~), and~~). They also continue to contribute toward the considerable uncertainty ~~to quantifications and interpretations of~~in quantifying and interpreting the ~~Earth's~~earth's changing radiation budget and hydrological cycles (Charlson et al., 1992; Ackerman et al., 2004; Boucher et al., 2013; Z. Li et al., 2011, 2017a; J. Guo et al., 2017~~; 2018~~, 2019a). Despite the great advances made in ~~observation~~the past decades in observational and modeling studies of ~~the~~ aerosol effects ~~in the past decades~~, it is still a challenge to accurately quantify ~~the~~aerosol effects on the climate system due to inadequate understanding of some mechanisms and strong variations in aerosol type, loading, and vertical distribution (Haywood and Boucher, 2000; Jacobson et al., 2001; Carslaw et al., 2013; J. Huang et al., 2015; J. Guo et al., 2016a; Z. Li et al., 2016; ~~Wang~~Wei et al., ~~2019~~2019a, 2019b). Aerosols ~~are known to~~can interact with thermodynamic stability through ARI (Atwater, 1971; Bond et al., 2013). Absorbing aerosols can stabilize the atmosphere (Ramanathan et al., 2001; Y. Wang et al., 2013; Ding et al., 2016~~), whereas they~~) and may also enhance convection and precipitation under certain conditions (Menon et al., 2002; Z. Li et al., 2017).

Thermodynamic stability in the planetary boundary layer (PBL) dictates the PBL development (~~Garret 1994;~~Stull, 1988; W. Zhang et al., 2018), thereby dominating the vertical dissipation of surface pollutants to some ~~degrees~~degree. Aerosols, in turn, have important feedbacks on the stability in the PBL, depending on ~~the~~ aerosol properties,

especially those of ~~the~~ light ~~absorption~~ absorbing aerosols (e.g., black, organic, and brown carbon). However, due to large uncertainties in aerosol radiative forcing, it remains a challenge to quantify the impact of aerosols on thermodynamic stability and PBL development. Conventionally, increasing the aerosol absorption tends to stabilize the atmosphere, leading to a reduced PBL height (PBLH). A more stable atmosphere and lower PBLH will, in turn, increase the surface aerosol loading, which is the well-established positive feedback loop in the aerosol-PBL interaction (e.g., H. Wang et al., 2015; Ding et al., 2016; Petäjä et al., 2016; Dong et al., 2017; Zou et al., 2017; Q. Huang et al., 2018; Z. Wang et al., 2018~~).~~; H. Wang et al., 2019). However, such a positive feedback loop may not be real for all situations and is subject to confounding factors such as aerosol type, aerosol vertical distribution, soil moisture, and PBL regime (J. Guo et al., ~~2019~~2019b; Lou et al., 2019). Geiß et al. (2017) reported the ambiguous ~~relationships~~relationship between surface aerosol loading and PBLH, while our previous study revealed weak correlations between surface pollutants and the PBLH in mountainous or clean regions (Su et al., 2018). ~~A recent study by~~ Lou et al. (2019) ~~shows~~showed that ~~aerosol has an even~~aerosols have a positive correlation with the PBLH under ~~the~~ stable PBL conditions, indicating the importance of thermodynamic conditions in the PBL ~~really matters~~.

Among others, numerical models are one of the viable methods used to determine ~~the~~ aerosol impacts on stability and PBL (e.g., J. Wang et al., ~~2014~~2014; Ding et al., 2016; Y. Wang et al., 2018; Zhou et al., 2018~~;~~). ~~Wang et al., 2014).~~ The aerosol optical ~~depths~~depth (AOD), a measure of aerosol columnar loading, is usually taken into

account in model simulations. However, the aerosol vertical distribution in models is generally prescribed and may differ ~~largely~~greatly from the real situation~~, which highly varies in the PBL and is closely linked to the significant uncertainties in aerosol radiative effects.~~. With observational constraints, the role of aerosol vertical ~~distribution~~distributions in aerosol-PBL interactions warrants ~~a~~ further investigation.

~~Coincidently, we have ample~~Ample observational datasets ~~over~~for Beijing are available, including aerosol vertical ~~distribution~~distributions derived from lidar, optical properties derived from ~~sun photometer,~~ the sunphotometer, profiles of meteorological variables from radiosonde (RS), ~~as well as~~and surface $PM_{2.5}$ and meteorological parameters. Based on these measurements, a radiative transfer model is used to simulate the vertical profiles of aerosol radiative forcing that are employed to investigate the impact of aerosols on ~~the~~ buoyancy in the lower atmosphere.

The paper is structured as follows~~:~~. Section 2 introduces the datasets and methods used. ~~The~~Section 3 presents analyses of aerosol-PBL ~~interaction~~interactions under different aerosol vertical structures ~~are presented in Section 3.~~. Section ~~5~~4 discusses the results with a brief summary.

2. Data and Method

2.1. Site description

~~In this study, we~~We utilized data from multiple sources in Beijing, a megacity located ~~at~~in the North China Plain. As one of the most densely populated and ~~well-~~urbanized regions in the world, Beijing is a polluted region with high concentrations of

absorbing aerosols (Y. Zhang et al., 2019). The micropulse lidar (MPL) located ~~at~~in Beijing was operated continuously by Peking University (39.99°N, 116.31°E) from ~~Mar~~March 2016 to ~~Dec~~December 2018, with a temporal resolution of ~~15s~~15 s and a vertical resolution of ~~15m~~15 m. Due to incomplete laser ~~pulses correction~~pulse corrections, the near-surface lidar blind ~~zones for lidar~~ zone is ~0.15 km. Background subtraction, saturation, after-pulse, overlap, and range corrections are applied to raw MPL data to calculate the normalized signals (Yang et al., 2013; Su et al., ~~2018). The~~2017a). MPL data on raining days are excluded. Level 1.5 AOD and single-scattering albedos (SSA) are employed at multiple wavelengths (i.e~~.~~., 0.44~~/~~, 0.5~~/~~, 0.67~~/~~, 0.87~~/~~, and 1.~~02μm~~02 μm) from the Beijing RADI (40°N, 116.38°E) Aerosol Robotic Network (AERONET) site ~~during~~from 2011~~–~~ to 2018~~, at~~ under cloud-free conditions (Holben et al., 1998; ~~Zhang et al., 2017;~~ Smirnov et al., 2000; Y. Zhang et al., 2017~~).~~). The ~~radiosonde (~~RS~~)~~ station (39.80°N, 116.47°E) ~~of~~in Beijing~~ is,~~ operated by the China Meteorological Administration, ~~which~~ is ~25 km from the MPL site. The variables observed at the RS station include ~~the meteorology~~meteorological data and profiles of water vapor, temperature, pressure, and wind. The vertical resolution of the RS is altitude dependent and generally less than 8 m (J. Guo et al., 2016b; W. Zhang et al., 2018). The RS is routinely launched at 0800 Local Time (LT) and 2000 LT ~~for~~ each day~~,~~ and is also ~~is~~ launched at 1400 LT in the summer (June-July-August). ~~The~~ RS measurements are collected during 2011–2018. To reduce small~~-~~-scale ~~bias~~biases and to obtain a ~~stable~~picture of the regional variation ~~of~~in particulate matter with the diameter smaller than 2.5 μm ($PM_{2.5}$), we acquire mean $PM_{2.5}$ data from twenty

environmental monitoring stations located within 20 km from the lidar site, including one station ~~of~~at the Beijing Embassy of the United States. ~~The~~Figure 1 shows the topography of Beijing ~~is presented in Figure 1~~. The green square indicates the MPL site, and the yellow triangle indicates the AERONET station. The brown star represents the ~~radiosonde (~~RS~~)~~ station, and the red pink dots represent the $PM_{2.5}$ sites.

2.2. Statistical analysis methods

~~Here the~~The statistical significance is tested by two independent statistical methods, namely, the least~~-~~-squares regression and the Kendall' tau (MK) test (Mann, 1945; Kendall, 1975~~).~~; J. Li et al., 2016). Least~~-~~-squares regression typically assumes a Gaussian data distribution in the trend analysis, whereas the MK test is a nonparametric test without any assumed functional form. The latter is more suitable for data that do not follow a certain distribution. To improve the robustness of the analysis, a relationship is considered ~~to be~~ significant when the confidence level is above 99% for both the least~~-~~-squares regression and the MK test. Hereafter, "significant" indicates that the correlation is statistically significant at the 99% confidence level.

~~In this study, we~~We primarily use the linear~~-~~-fit method to build ~~the~~ relationships between different parameters~~, and the~~. The Pearson correlation coefficient derived from the linear regression analysis measures the degree to which the data fit a linear relationship. However, following our recent work (Su et al., 2018), ~~the~~ inverse fitting ~~([~~$f(x) = A/x + B$~~)]~~ is used to establish the relationship between PBLH and $PM_{2.5}$. ~~During this time, the~~The magnitude of the correlation coefficient ($R^{\dagger}$) is designed to measure the degree to which the data fit an inverse relationship. Since the relationship

between the PBLH and $PM_{2.5}$ is non-linear, the inverse fitting ~~is more suitable to characterize~~better characterizes this relationship.

2.3. PBLH and buoyancy derived from RS

The RS vertical resolution varies according to the balloon ascending rate~~, and~~. The RS ~~is recorded~~records measurements every 1.~~2s~~2 s, which represents an approximate vertical resolution of 5–8 m. Prior to the retrieval of the PBLH, we further resample ~~the radiosonde~~RS data to achieve a vertical resolution of 5~~-~~ hPa with linear interpolation. We follow a well-established method developed by Liu and Liang (2010) to derive the PBLH based on ~~the~~ profiles of the potential temperature gradient that takes into account ~~of~~ different stability conditions. In this study, we only focus on ~~PBL~~PBLs driven by buoyancy, ~~and thus, the PBL~~so PBLs driven by ~~the~~ low-level jets ~~will be~~are excluded using ~~the~~RS-derived wind profiles ~~from radiosonde~~ (Liu and Liang, 2010; Miao et al., 2018).

The static stability ~~in~~of the atmosphere is determined by the buoyancy force, which ~~can be~~is expressed as (Wallace and Hobbs, 2006~~):~~)

$$B = \frac{d^2z}{dt^2} = \frac{T' - T}{T} g = -g\Delta z \frac{1}{\theta}\frac{d\theta}{dz} \quad , \qquad (1)$$

where z is the height of the air parcel, and t indicates the time. T' represents the temperature of the parcel ~~and~~, T represents the temperature of the environment, and θ is the virtual potential temperature of the environment. ~~For a certain~~An atmospheric layer~~, the atmosphere is identified as a~~ is convective ~~condition when~~if the buoyancy is above zero~~, but is identified as a~~ and stable ~~condition~~ when the buoyancy is below zero. If the buoyancy is near zero, the atmosphere is ~~under a~~ neutral ~~condition~~. Based

Formatted: Font: Italic
Formatted: Space Before: 0.1 line
Formatted: Font: Italic
Formatted: Font color: Auto
Formatted: Font color: Auto

on the identification method for PBL ~~types~~type (Liu and Liang, 2010; W. Zhang et al., 2018), we present profiles of buoyancy forcing for ~~a~~ stable, neutral, and convective ~~PBL~~PBLs (Figure 2a). ~~Clearly, the~~Results shown are averages from 3069 radiosonde measurements, of which 438 cases are convective PBLs, 714 cases are neutral PBLs, and 1916 cases are stable PBLs. The strongest upward or downward forcing occurs near the surface. ~~Figure~~Figures 2b-c further show the height~~-~~-dependent correlation coefficients between buoyancy and PBLH/$PM_{2.5}$ with an interpolation window of 0.~~2km. Noted~~2 km. Note that the PBLH and surface $PM_{2.5}$ are fixed for the entire column, and the buoyancy is height~~-~~dependent. Due to the insufficient development of the PBL, we do not use RS data at 0800 LT here. To exclude the impact induced by the dragging effects of rainfall, we only ~~use the~~consider cases without precipitation within the past 24 hours. Strong upward buoyancy can uplift the PBLH and mitigate ~~the~~ surface pollutants, especially in the ~~low~~lower atmosphere. Thus, we integrate the buoyancy forcing within the lowest ~~1km~~1 km (red line in ~~Figure~~Figures 2b-c), ~~which is~~ defined as the ~~low~~lower-atmosphere buoyancy (LAB). As shown in ~~Figure~~Figures 3a-b, ~~the~~ LAB ~~shows strong negative correlations with~~ and $PM_{2.5}$ ~~but positive correlations with~~ are negatively correlated, and LAB and PBLH~~. The~~ are positively correlated. LAB also has a significant negative ~~correlations~~correlation with absorbing aerosol optical depth~~. It could~~ (Figure 3c). This may be ~~partly caused by~~due to the stabilizing effect of absorbing ~~aerosol~~aerosols on the atmosphere, ~~which is~~ widely reported in many previous studies (H. Wang et al., 2015; Ding et al., 2016; Petäjä et al., 2016; Dong et al., 2017; Z. Li et al., ~~2017~~2017b; X. Huang et al., 2018).

2.4. PBLH and aerosol extinction coefficient derived from MPL

MPL data from Beijing were used to retrieve the PBLH during the daytime (0800–1900 LT). ~~Multiple~~Many methods have been developed for retrieving the PBLH from MPL measurements, ~~such as~~e.g., the signal threshold (Melfi et al., 1985), the maximum of the signal variance (Hooper and Eloranta, 1986), the minimum of the signal profile derivative (Flamant et al., 1997), and the wavelet transform (Cohn and Angevine, 2000; Davis et al., 2000; Su et al., ~~2017~~2017b; Chu et al., 2019). To derive the PBLH from MPL data, we adopted previous well-established approaches with several refinements, which ~~has~~have already been validated by long-term data ~~over~~collected at the Southern Great Plains ~~(ARM SGP)~~ site (Sawyer and Li, 2013; Su et al., ~~2019~~2020).

~~Initially, we~~We initially identify the local maximum positions (range: 0.25~~–4km~~ 4 km) in the covariance transform function collocated with a signal gradient larger than a certain threshold. We further estimated the shot noise (σ) induced by background light and dark ~~current~~currents for each profile, and then set the ~~certain~~ threshold as~~–~~ 3σ. The initial PBLH retrieval (~~0800LT~~at 0800 LT) is constrained by the PBLH value derived from the morning RS sounding. Then, the following PBLHs ~~would be~~are retrieved using a stability~~–~~dependent model based on continuity. ~~The boundary~~Boundary layer clouds are identified to diagnose the PBLH for cloudy cases. Figure 3d presents the comparison of summertime PBLH results derived from MPL and RS at 1400 LT, ~~and the~~showing good agreement ~~is reasonably good~~ (R = 0.79).

Multiple studies have provided a well-established algorithm to retrieve the vertical profiles of aerosol extinction coefficient (AEC) from MPL ~~(eg~~data (e.g., Fernald, 1984;

Klett, 1985; Liu et al., 2012). ~~Then, the~~The Klett method is further ~~applied for retrieving~~used to retrieve extinction profiles (Klett, 1985). The column-averaged extinction-to-backscatter ratio (the so-called lidar ratio) is an important parameter in the retrieval ~~processes~~process and is constrained using AERONET-derived AOD at 0.~~5μm derived from AERONET.~~5 μm. The AEC is assumed to be equal within the blind zone. The overall uncertainties from the overlap function, the lidar ratio, the effects of multiple scattering, and ~~noises are estimated to~~noise fall within ~~a~~the range of 20~~–~~–30% in the retrieval ~~processes~~process (He et al., 2006).

2.5. Estimation of the impacts of aerosols on buoyancy

To ~~illustrate the~~show vertical ~~profile~~profiles of aerosol radiative forcing, the Santa Barbara DISORT Atmospheric Radiative Transfer (SBDART) model (Ricchiazzi et al., 1998) was used to simulate the atmospheric heating rate (dT/dt) induced by ~~aerosol~~aerosols (Liu et al., 2012; Dong et al., 2017). ~~The integrated~~Integrated aerosol inputs include AODs, ~~and~~ SSAs (i.e., at 0.44, 0.67, 0.87, and 1.~~02μm~~02 μm) retrieved from AERONET measurements, ~~as well as the~~ and AEC profiles at 0.~~5μm~~5 μm obtained from the MPL. We also use ~~the MODIS~~Moderate Resolution Imaging Spectroradiometer surface ~~reflectance~~reflectances as ~~the~~an additional ~~inputs~~input (https://modis.gsfc.nasa.gov/data/dataprod/mod09.php). —We further use heating ~~rate~~rates induced by aerosols to estimate the ~~impacts~~impact of aerosols on buoyancy.

Theoretically, the rate of change in buoyancy for a certain layer ~~can be~~is expressed as~~:~~

$$\frac{dB}{dt} = \frac{d}{dt}\left(\frac{T_0 - \Gamma_d \Delta z - T}{T} g\right) = \frac{\left(\frac{dT_0}{dt} - \frac{dT}{dt}\right) T + \frac{dT}{dt}(\Gamma_d - \Gamma)\Delta z}{T^2} g \quad , \qquad (2)$$

where most parameters are defined in the same way as in Eq. (1), and Γ_d (Γ) represents the dry adiabatic lapse rate (environmental lapse rate). We ~~will~~ primarily focus on the rate of change ~~rate~~ in buoyancy during the noontime period (1100~~–1500LT~~–1500 LT), when the PBL is well developed, and aerosol radiative forcing is strong. The rate of change ~~rate~~ in buoyancy (dB/dt) induced by aerosols is largely determined by the aerosol heating rate, which can be produced by the radiative transfer model. Additional inputs include the environmental lapse rate and temperature, ~~which are~~ obtained from noontime RS soundings in the summer. For other times, the environmental lapse rate and temperature are obtained from MERRA-2 reanalysis data, which assimilates coarse-resolution RS ~~observation~~observations (Rienecker et al., 2011). In this way, we can estimate dB/dt induced by aerosols with a primary focus on the daytime. ~~Noted~~Note that the errors in MERRA-2 data ~~would~~ lead to ~~the~~ uncertainties in the ~~estimated dB~~estimateddB/dt. A 1~~–~~–3 K ~~uncertainties~~uncertainty in MERRA-2 ~~temperature~~temperatures (Gelaro et al., 2017) ~~lead~~leads to 1~~–~~–3% relative biases in the estimated dB/dt. Considering the large variation in dB/dt ~~under~~for different aerosol structures, the biases resulting from MERRA-2 data are not a ~~very~~ serious issue.

3. Results

3.1. Classification of different aerosol structure scenarios

By altering the adiabatic heating rate of the atmosphere, the aerosol vertical

distribution is of great importance to the PBL. Based on cloud-free AEC profiles in the PBL, aerosol vertical structures can be classified into three types: well-mixed, decreasing with height, and its inverse~~.~~, increasing with height. If AEC varies by less than 20% within the lowest 80% of the PBL, it is considered a well-mixed structure. For the other cases, a decreasing structure indicates a peak in AEC near the surface, and the inverse structure indicates a peak in AEC in the middle or upper PBL.

To investigate the vertical variation ~~of~~in AEC within the PBL, the evolution of the PBLH has ~~been~~to be taken into account. Following previous studies (~~Kuang et al., 2017;~~ Ferrero et al., 2014~~), the~~; Kuang et al., 2017), vertical profiles were normalized by introducing a standardized height (H_s), ~~which was~~ calculated as follows:

$$H_s = \frac{z - PBLH}{PBLH} \quad , \qquad (3)$$

where z is the height above the ground, and H_s is 0 at the PBL top and -1 at ground level. ~~Then,~~Figure 4 shows the normalized vertical profiles of AEC ~~during~~derived from MPL data for different aerosol structures around noontime. The number of samples and percentages of decreasing, well-mixed, and increasing aerosol structures are ~~shown in Figure 4~~998 (51%), 611 (32%), and 330 (17%), respectively. Since a temperature inversion located at the PBL top traps moisture and aerosols, there is a sharp decrease in the AEC profile from the PBL upper boundary to the free atmosphere. ~~The~~Variations in the aerosol vertical distribution largely ~~varies depending~~depend on different conditions, but share similar features ~~under~~among the different aerosol structure patterns. Despite complex aerosol vertical distributions, these three types of profiles can account for most of the cloud-free cases.

Formatted: Space Before: 0.1 line

Formatted: Font: Italic

3.2. PBLH and $PM_{2.5}$ under different aerosol structure scenarios

Absorbing aerosols ~~trend~~tend to have a positive feedback with the PBLH, ~~while aerosols~~ and the aerosol vertical distribution plays a critical role in this process. We investigate the relationship between MPL-derived PBLH and $PM_{2.5}$ for absorbing (daily average SSA $\leq$ 0.85) or weakly absorbing (daily average SSA > 0.9) aerosols ~~under inverse/declining~~ for increasing/decreasing aerosol structures during 0900–1900 LT (Figure 5). The PBLH-$PM_{2.5}$ relationships can represent the intensity of the aerosol-PBL interaction. In general, there are stronger correlations between PBLH and $PM_{2.5}$ ~~under~~for the inverse ~~aerosols~~aerosol structure. ~~Under such structure, the PBLH-$PM_{2.5}$ correlation also remains considerably stronger for absorbing than weakly absorbing cases.~~ This is likely caused by substantial heating in the upper PBL, ~~which would facilitate~~facilitating the formation of a temperature inversion and further ~~increase~~increasing the stability ~~in~~of the PBL. ~~While, under declining aerosols~~For the decreasing aerosol structure, ~~the~~ aerosols may not significantly redistribute ~~the~~ adiabatic energy. ~~This phenomenon indicates~~Hence, the PBLH-$PM_{2.5}$ correlation is relatively weak. Significant PBLH-$PM_{2.5}$ correlations are found for both absorbing and weakly absorbing cases, indicating that ~~the absorbing aerosol could~~ scattering aerosols may also play ~~a more~~an important role in the aerosol-PBL interaction, especially for the inverse aerosol structure.

~~The~~Figure 6 presents the averaged diurnal cycles of AEC, PBLH, and $PM_{2.5}$ for different aerosol vertical structures ~~are presented in Figure 6~~, classified based on the ~~measurements made in Beijing.~~average AEC profiles during noontime. High humidity

cases (surface relative humidity > 90%) and strong wind cases (wind speed > 5m s^{-1}) are excluded. ~~Theoretically~~Here, both AEC and PBLH are derived from MPL data. Data are collected on 371 available days, of which 191 days have decreasing aerosol structures, 122 days have well-mixed aerosol structures, and 58 days have inverse aerosol structures. Multiple entangled factors can contribute to the formation of different aerosol structures within the PBL, including synoptic patterns, new particle formation, vertical turbulence, horizontal transport, entrainment rates, to name a few. In general, the inverse structure is characterized by higher aerosol loadings and lower PBLHs, whereas the decreasing structure is characterized by light pollution and a well-developed PBL. In theory, $PM_{2.5}$ should generally decrease with increasing PBLH in the morning ~~and forenoon~~ due to the dilution effect. This situation is demonstrated clearly for decreasing aerosol structures. However, $PM_{2.5}$ continuously grows during the daytime ~~under~~when an inverse aerosol ~~structures~~structure is present, regardless of the PBLH diurnal cycle. ~~Despite~~Even though many factors control the diurnal variations ~~of aerosol~~in aerosols and the PBL ~~are controlled by many factors~~, the strong aerosol-stability interaction ~~may be an underlying scheme that further enhances~~generates an unfavorable condition for the vertical dissipation of aerosols, so the surface aerosol loading ~~during the daytime~~can continuously accumulate due to emissions.

The correlations and statistical results concerning the PBLH and $PM_{2.5}$ provide hints about the differences in aerosol-PBL interactions for different aerosol structures. However, these results cannot explain the feedback loop and causality. Therefore, we

further use the SBDART model with the constraint of ample observations to investigate the vertical profiles of radiative forcing induced by aerosols and its impacts on atmospheric stability.

3.3. Aerosol radiative forcing for different aerosol structures

Following the description in Section 2.5, we calculate the statistical means of aerosol radiative forcing in the vertical for decreasing, well-mixed, and inverse aerosol structures, derived from the cases~~. The~~ presented in Figure 6. Figure 7 shows that the vertical distributions of the heating rate differ drastically ~~with significant heating in~~among the different ~~parts of PBL. This is caused by~~aerosol structures. For the inverse aerosol structure scenario, aerosols cause substantial heating in the upper PBL, ~~which would facilitate~~facilitating the formation of a temperature inversion and further ~~increase the stability in the PBL. Nonetheless, under the declining aerosol structure, the abundant aerosols~~ increasing the stability in the PBL. For the decreasing aerosol structure scenario, the abundance of aerosols at the bottom of PBL ~~can cause a heating effect in~~heats the lower PBL~~, and hence,~~ so can potentially enhance ~~the~~ convection in the PBL.

There are considerable differences in heating rate among the three distinct aerosol structures (Figure 8), which affects the atmospheric buoyancy and stability differently. On average, aerosols generally suppress buoyancy in the ~~low~~lower atmosphere. Such an effect is quite notable for the inverse structure and is insignificant for the decreasing structure with large standard deviations. Absorbing ~~aerosol is~~aerosols are not very helpful for stabilizing ~~low~~ the lower atmosphere ~~under the~~when a decreasing aerosol

structure is present, but ~~plays~~they play an important role ~~under the~~when an inverse aerosol structure is present. As such, we ~~expected~~expect the strongest aerosol-PBL ~~interactions~~interaction to occur for absorbing aerosol cases ~~under the~~when an inverse aerosol structure~~, which~~ is present, consistent with the results shown in Figure ~~4. It should be noted that there are large variations in the impact of aerosol on buoyancy. Under an inverse structure, aerosol overwhelmingly enhance the stability in low-atmosphere, whereas, under decreasing structure, aerosols have the potential to either enhance or suppress the low-atmosphere stability depending on different cases~~5.

Figure 9 ~~illustrates the~~shows schematic ~~diagram~~diagrams of the interactions between aerosols, stability, and the PBL~~.~~ when decreasing/inverse aerosol structures are present. Overall, ~~aerosol~~ both decreasing and inverse aerosol structures can cool the surface and suppress sensible heat, thus stabilizing the PBL. In both cases, aerosols have notable stabilizing effects near the surface.

When a decreasing aerosol structure is present, abundant aerosols near the surface generate a stronger aerosol heating rate in the lower PBL than in the upper PBL. Such aerosol radiative forcing lowers the potential temperature gradient ($d\theta/dz$) in the middle and upper PBL and can further strengthen vertical ~~structure critically affects the~~ convection in the middle and upper PBL. The opposite aerosol effects on PBL stability lead to a relatively weak aerosol feedback and a relatively weak aerosol-PBL interaction. ~~The~~When an inverse aerosol structure is present, the significant heating effect on the upper PBL facilitates the formation of temperature inversion and further increases the stability and ~~aerosol loading in the near surface. Therefore, the inverse aerosol structure~~

Formatted: Font color: Black

Formatted: Font color: Black

Formatted: Font color: Black

~~may strengthen the aerosol-PBL interaction. Meanwhile, the aerosol-PBL interaction can be potentially neutralized by the decreasing structure. Moreover, aerosols can both enhance and suppress the PBL stability depending on different conditions, and lead to both~~ suppresses the PBLH. The notable increase in stability lead to the strong, positive ~~and negative feedback loops (Figure 9).~~aerosol feedback.

Highly variable aerosol vertical distributions cause large variations in the impact of aerosol on stability, and thus, exert important and highly variable influences on the aerosol-PBL interactions. Although aerosol stabilize PBL for majority cases, aerosol also can suppress the stability in low-atmosphere when aerosol heating effect is much stronger on the near surface than upper PBL, and further lead to a potential negative feedback loop. The positive feedback loop leads to strong aerosol-PBL interactions, ~~while the~~whereas negative feedback loop ~~partly offset PBL's impacts on~~leads to weak aerosol ~~loading~~ PBL interactions. It explains the paradox of the ~~impact of the PBL on~~ different correlations between PBLH and surface pollutants~~,~~ since its magnitude, significance, and even sign reportedly varies or even reverses (Quan et al., 2013; Tang et al., 2015; Geiß et al., 2017; Su et al., 2018).

Formatted: Space Before: 6 pt

Formatted: Font color: Black

4. Summary and Discussion

Based on integrated aerosol and meteorological measurements ~~over~~made in Beijing, the aerosol-PBL interaction is assessed ~~under~~for different aerosol vertical structures, ~~which are~~i.e., decreasing, well~~-~~ mixed, and inversely increasing with height~~,~~ ~~respectively~~. The aerosol-PBL relationships and the diurnal cycles of PBLH and $PM_{2.5}$

show distinct characteristics among the different aerosol vertical patterns. For the decreasing aerosol structure, $PM_{2.5}$ decreases in the morning ~~and forenoon~~ with relatively large PBLH growth rates. In this situation, absorbing ~~aerosol is~~aerosols are not very helpful in stabilizing ~~low~~ the lower atmosphere. ~~Under~~For the inverse aerosol structure, $PM_{2.5}$ continuously grows during the daytime with ~~relative~~relatively low PBLH growth ~~rate~~rates. This phenomenon could be a sign of ~~the~~a strong aerosol-PBL interaction. The aerosol radiative forcing in the vertical ~~scale~~ for decreasing, well-mixed, and inverse aerosol structures differ drastically with strong heating in the lower, ~~mid~~middle, and upper PBL, respectively. Such a difference in heating rate affects the atmospheric buoyancy and stability differently in the three distinct aerosol structures.

~~Numerous studies used various models~~Turbulent fluxes and eddies in the PBL would spread out and redistribute the radiative effects induced by aerosols. Needed are numerical models to ~~simulate~~quantify the aerosol-PBL ~~interactions~~interaction and consequent feedbacks (e.g., Y. Wang et al., ~~,~~2013; Ding et al., 2016; Z. Wang et al., 2018; Zhou et al., 2018~~; Wang et al., 2014~~). Aerosol vertical ~~distribution highly varies in~~ distributions greatly vary on both temporal and vertical scales~~,~~ and critically affect ~~the~~ aerosol radiative ~~forcing. Nonetheless~~effects. However, the aerosol vertical distribution ~~usually~~is still poorly represented in numerical models, partly due to a lack of observational constraints. This study reveals the important role of the aerosol vertical distribution in the aerosol-PBL ~~interactions~~interaction, which should be carefully taken into account in both observational ~~analysis~~analyses and model simulations.

~~In this~~This study~~, we use~~ used column-averaged aerosol properties from

AERONET. However, the vertical variations ~~of single scattering albedo~~in SSA and aerosol type remains unknown, ~~which can induce~~inducing uncertainties in the estimation of aerosol effects. In the future, we plan to use aircraft data from field campaigns to better account for ~~its influences for~~ the influence of different types of aerosols ~~of~~with different properties.

Data availability. ~~The hourly~~Hourly $PM_{2.5}$ data are released by the Ministry of Environmental Protection of China ~~(data link:~~ (http://113.108.142.147:20035/emcpublish). ~~The~~ MERRA-2 reanalysis data are publicly available at https://disc.gsfc.nasa.gov/datasets?keywords=merra%202&page=1. ~~The~~ AERONET data are publicly available at https://aeronet.gsfc.nasa.gov. ~~The meteorological~~ Meteorological data are provided by the data center of the China Meteorological Administration (~~data link:~~ http://data.cma.cn/en).

Author contribution. T. S. and Z. L. conceptualized this study. T. S. carried out the analysis, with comments from other co-authors. C. L., J. L~~.~~., and W. T. carried out the MPL ~~observation~~observations. J. G. provided auxiliary data. W. H., C. S., W. T., J. W., and J. G. provided useful suggestions for the ~~discussion~~study. T. S. and Z. L. interpreted the data and wrote the manuscript with contributions from all co-authors.

Formatted: Font color: Auto

Competing interests. The authors declare that they have no conflict of interest.

Acknowledgements. This work is supported in part by grants from the National Science Foundation (AGS1837811 and AGS1534670). The authors would like to acknowledge Prof. Zhengqiang Li for his effort in establishing and maintaining the Beijing RADI AERONET site. We thank the provision of $PM_{2.5}$ data by the Ministry of Environmental Protection of the People's Republic of China, and also thank the provision of meteorological data and radiosonde data by the China Meteorological Administration. We extend sincerest thanks to the MERRA teamsteam for their datasets.

Formatted: Heading 1

References

Ackerman, A. S., Kirkpatrick, M. P., Stevens, D. E., and Toon, O. B., 2004.: The impact of humidity above stratiform clouds on indirect aerosol climate forcing. Nature, 432, 1014–1017. https://doi.org/10.1038/nature03174., 2004.

Atwater, M. A., 1971.: The radiation budget for polluted layers of the urban environment. Journal of Applied Meteorology, 10(2), 205–214., 1971.

Bond, T. C., Doherty, S. J., Fahey, D. W., Forster, P. M., Berntsen, T., DeAngelo, B. J., Flanner, M. G., Ghan, S., Kärcher, B., Koch, D. and Kinne, S., 2013.: Bounding the role of black carbon in the climate system: A scientific assessment. Journal of Geophysical Research: Atmospheres, 118(11), 5380–5552., 2013.

Boucher, O., Randall, D., Artaxo, P., Bretherton, C., Feingold, G., Forster, P., Kerminen, V. M., Kondo, Y., Liao, H., Lohmann, U., and Rasch, P., 2013.: Clouds and aerosols, in: Climate Change 2013: The Physical Science Basis. Contribution of Working Group I to the Fifth Assessment Report of the Intergovernmental Panel on Climate Change, 571–657, Cambridge Univ. Press, Cambridge, UK and New York, NY, USA., 2013.

Carslaw, K.S., Lee, L.A., Reddington, C.L., Pringle, K.J., Rap, A., Forster, P.M., Mann, G.W., Spracklen, D.V., Woodhouse, M.T., Regayre, L.A. and Pierce, J.R., 2013.: Large contribution of natural aerosols to uncertainty in indirect forcing. Nature, 503(7474), p.67., 2013.

Charlson, R.J., Schwartz, S.E., Hales, J.M., Cess, R.D., Coakley, J.J., Hansen, J.E. and Hofmann, D.J., 1992.: Climate forcing by anthropogenic aerosols. Science, 255(5043), pp.423-430, 1992.

Chu, Y., Li, J., Li, C., Tan, W., Su, T. and Li, J.: Seasonal and diurnal variability of planetary boundary layer height in Beijing: Intercomparison between MPL and WRF results. Atmospheric Research, 227, pp.1-13. https://doi.org/10.1175/1520-0450(2000)039<1233:BLHAEZ>2.0.CO;2, 2000, 2019.

Cohn, S. A. and Angevine, W. M.: Boundary layer height and entrainment zone thickness measured by lidars and wind-profiling radars, J. Appl. Meteorol., 39, 1233–1247, https://doi.org/10.1175/1520-0450(2000)039<1233:BLHAEZ>2.0.CO;2, 2000.2000.

Davis, K. J., Gamage, N., Hagelberg, C. R., Kiemle, C., Lenschow, D. H., and Sullivan P. P.: An objective method for deriving atmospheric structure from airborne lidar observations. J. Atmos. Ocean. Tech., 17, 1455–1468, https://doi.org/10.1175/1520- 0426(2000)017<1455:AOMFDA>2.0.CO;2, 2000

Deardorff, J. W., G. E. Willis, and B. H. Stockton.: Laboratory studies of the entrainment zone of a convectively mixed layer. J. Fluid. Mech., 100, 41–64, doi: 10.1017/ S0022112080001000, 1980.

Ding, A.J., Huang, X., Nie, W., Sun, J.N., Kerminen, V.M., Petäjä, T., Su, H., Cheng, Y.F., Yang, X.Q., Wang, M.H. and Chi, X.G., 2016.: Enhanced haze pollution by black carbon in megacities in China. Geophysical Research Letters, 43(6), pp.2873-2879., 2016.

Dong, Z., Li, Z., Yu, X., Cribb, M., Li, X., and Dai, J.: Opposite long-term trends in aerosols between low and high altitudes: a testimony to the aerosol–PBL feedback, Atmos. Chem. Phys., 17, 7997–8009, https://doi.org/10.5194/acp-17- 7997-2017, 2017.

Fernald, F.G., 1984.: Analysis of atmospheric lidar observations: some comments. Applied optics, 23(5), pp.652-653, 1984.

Ferrero, L., Castelli, M., Ferrini, B.S., Moscatelli, M., Perrone, M.G., Sangiorgi, G., D'Angelo, L., Rovelli, G., Moroni, B., Scardazza, F. and Močnik, G., 2014.: Impact of black carbon aerosol over Italian basin valleys: high-resolution measurements along vertical profiles, radiative forcing and heating rate. Atmospheric Chemistry and Physics, 14(18), pp.9641-9664., 2014.

Flamant, C., Pelon, J., Flamant, P.H. and Durand, P., 1997.: Lidar determination of the entrainment zone thickness at the top of the unstable marine atmospheric boundary layer. Boundary-Layer Meteorology, 83(2), pp.247-284, 1997.

Geiß, A., Wiegner, M., Bonn, B., Schäfer, K., Forkel, R., Schneidemesser, E.V., Münkel, C., Chan, K.L. and Nothard, R., 2017.: Mixing layer height as an indicator for urban air quality?. Atmospheric Measurement Techniques, 10(8), pp.2969-2988., 2017.

Gelaro, R., McCarty, W., Suárez, M.J., Todling, R., Molod, A., Takacs, L., Randles, C.A., Darmenov, A., Bosilovich, M.G., Reichle, R. and Wargan, K., 2017.: The modern-era retrospective analysis for research and applications, version 2 (MERRA-2). Journal of Climate, 30(14), pp.5419-5454, 2017.

Guo, J., H. Liu, F. Wang, J. Huang, F. Xia, M. Lou, Y. Wu, J. Jiang, T. Xie, Y. Zhaxi, and Y. Yung, 2016.: Three-dimensional structure of aerosol in China: A perspective from multi-satellite observations, Atmospheric Research, 178–179:

Formatted: Font: Calibri, 10.5 pt

Formatted: Font: Calibri, 10.5 pt

pp.580–589, 2016a.
Guo, J.,Guo, J., Miao, Y., Zhang, Y., Liu, H., Li, Z., Zhang, W., He, J., Lou, M., Yan, Y., Bian, L., and Zhai, P., 2016.: The climatology of planetary boundary layer height in China derived from radiosonde and reanalysis data. Atmospheric Chemistry and Physics, 16, pp.13309–13319., 2016b.
Guo, J., Su, T., Li, Z., Miao, Y., Li, J., Liu, H., Xu, H., Cribb, M. and Zhai, P., 2017.: Declining frequency of summertime local-scale precipitation over eastern China from 1970 to 2010 and its potential link to aerosols. Geophysical Research Letters, 44(11), pp.5700-5708., 2017.
Guo, J., Su, T., Chen, D., Wang, J., Li, Z., Lv, Y., Guo, X., Liu, H., Cribb, M. and Zhai, P.: Declining summertime local-scale precipitation frequency over China and the United States, 1981–2012: The disparate roles of aerosols. Geophysical Research Letters, 2019a.
Guo, J., Y. Li, J. Cohen, J. Li, D. Chen, H. Xu, L. Liu, J. Yin, K. Hu, P. Zhai, 2019.: Shift in the temporal trend of boundary layer height trend in China using long-term (1979–2016) radiosonde data. Geophysical Research Letters, 46 (11), pp.6080-6089, 2019b.
Haywood, J. and Boucher, O., 2000.: Estimates of the direct and indirect radiative forcing due to tropospheric aerosols: A review. Reviews of geophysics, 38(4), pp.513-543., 2000.
He, Q.S., Li, C.C., Mao, J.T., Lau, A.K.H. and Li, P.R., 2006.: A study on the aerosol extinction-to-backscatter ratio with combination of micro-pulse LIDAR and MODIS over Hong Kong. Atmospheric Chemistry and Physics, 6(11), pp.3243-3256., 2006.
Holben, B.N., Eck, T.F., Slutsker, I., Tanre, D., Buis, J.P., Setzer, A., Vermote, E., Reagan, J.A., Kaufman, Y.J., Nakajima, T. and Lavenu, F., 1998.: AERONET—A federated instrument network and data archive for aerosol characterization. Remote sensing of environment, 66(1), pp.1-16., 1998.
Hooper, W. P. and Eloranta, E. W.: Lidar measurements of wind in the planetary boundary layer – the method, accuracy and results from joint measurements with radiosonde and kytoon, Bound.- Lay. Meteorol., 25, 990–1001, 1986.
Huang, J., J. Guo, F. Wang, Z. Liu, M. -J. Jeong, H. Yu and Z. Zhang, 2015.: CALIPSO inferred most probable heights of global dust and smoke layers, Journal of Geophysical Research-Atmospheres, 120(10), pp5085–5100, 2015.
Huang, Q., Cai, X., Wang, J., Song, Y. and Zhu, T., 2018.: Climatological study of the Boundary-layer air Stagnation Index for China and its relationship with air pollution. Atmospheric Chemistry and Physics, 18(10), p.7573., 2018.
Huang, X., Wang, Z. and Ding, A., 2018.: Impact of Aerosol-PBL Interaction on Haze Pollution: Multiyear Observational Evidences in North China. Geophysical Research Letters, 45(16), pp.8596-8603., 2018.
Jacobson, M.Z.: Strong radiative heating due to the mixing state of black carbon in atmospheric aerosols. Nature, 409(6821), p.695, 2001.
Kendall, M. G.: Rank Correlation Methods, 1–202, Griffin, London, 1975.
Klett, J.D., 1985.: Lidar inversion with variable backscatter/extinction ratios. Applied

optics, 24(11), pp.1638-1643, 1985.
Kuang, Y., Zhao, C.S., Tao, J.C., Bian, Y.X. and Ma, N., 2016.: Impact of aerosol hygroscopic growth on the direct aerosol radiative effect in summer on North China Plain. Atmospheric Environment, 147, pp.224-233., 2016.
Li Z. et al. 2007: Preface to special section on East Asian Study of Tropospheric Aerosols: an International Regional Experiment (EAST-AIRE), J. Geophys. Res., D22S00, doi:10.1029/2007JD008853.
Zhu, 2017b. Aerosol and boundary-layer interactions and impact on air quality. National Science Review, nwx117. https://doi.org/10.1093/nsr/nwx117.
Li, J., Li, C., Zhao, C. and Su, T.: Changes in surface aerosol extinction trends over China during 1980 – 2013 inferred from quality - controlled visibility data. Geophysical Research Letters, 43(16), pp.8713-8719, 2016.
Li, Z., Niu, F., Fan, J., Liu, Y., Rosenfeld, D. and Ding, Y., 2011.: Long-term impacts of aerosols on the vertical development of clouds and precipitation. Nature Geoscience, 4(12), p.888., 2011.
Li, Z., W.K.-M. Lau, V. Ramanathan, et al.: Aerosol and monsoon climate interactions over Asia. Rev. of Geophys., 54, 866–929. https://doi.org/10.1002/2015RG000500, 2016.
Li, Z., Rosenfeld, D., and Fan, J., 2017a.: Aerosols and their Impact on Radiation, Clouds, Precipitation and Severe Weather Events, Oxford Encyclopedia in Environmental Sciences, 10.1093/acrefore/9780199389414.013.126, 2017a.
Li, Z., J. Guo, A. Ding, H. Liao, J. Liu, Y. Sun, T. Wang, H. Xue, H. Zhang, B. Zhu.: Aerosol and boundary-layer interactions and impact on air quality. National Science Review, nwx117. https://doi.org/Li, Z., W.K.-M. Lau, V. Ramanathan, et al., 2016. Aerosol and monsoon climate interactions over Asia. Rev. of Geophys., 54, 866–929. https://doi.org/10.1002/2015RG000500.
10.1093/nsr/nwx117, 2017b.
Liu, S. and Liang, X.-Z.: Observed diurnal cycle climatology of planetary boundary layer height, J. Climate, 22, 5790–5809, https://doi.org/10.1175/2010JCLI3552.1, 2010.
Liu, J., Zheng, Y., Li, Z., Flynn, C. and Cribb, M., 2012.: Seasonal variations of aerosol optical properties, vertical distribution and associated radiative effects in the Yangtze Delta region of China. Journal of Geophysical Research: Atmospheres, 117(D16).), 2012.
Lou, M., J. Guo, L. Wang, H. Xu, D. Chen, Y. Miao, Y. Lv, Y. Li, X. Guo, S. Ma, and J. Li, 2019.: On the relationship between aerosol and boundary layer height in summer in China under different thermodynamic conditions. Earth and Space Science, 6(5), pp.887-901, 2019.
Mann, H. B.: Nonparametric tests against trend, Econometrica, 13, 245–259, 1945.
Melfi, S.H., Spinhirne, J.D., Chou, S.H. and Palm, S.P., 1985.: Lidar observations of vertically organized convection in the planetary boundary layer over the ocean. Journal of climate and applied meteorology, 24(8), pp.806-821., 1985.
Menon, S., Hansen, J., Nazarenko, L. and Luo, Y., 2002.: Climate effects of black carbon aerosols in China and India. Science, 297(5590), pp.2250-2253., 2002.

Miao, Y., Guo, J., Liu, S., Wei, W., Zhang, G., Lin, Y. and Zhai, P., 2018.: The climatology of low‐level jet in Beijing and Guangzhou, China. Journal of Geophysical Research: Atmospheres, 123(5), pp.2816-2830, 2018.

Petäjä, T., Järvi, L., Kerminen, V.M., Ding, A.J., Sun, J.N., Nie, W., Kujansuu, J., Virkkula, A., Yang, X., Fu, C.B., Zilitinkevich, S., and M. Kulmala., 2016.: Enhanced air pollution via aerosol-boundary layer feedback in China. Scientific Reports, 6. https://doi.org/10.1038/srep18998., 2016.

Quan, J., Gao, Y., Zhang, Q., Tie, X., Cao, J., Han, S., Meng, J., Chen, P. and Zhao, D., 2013.: Evolution of planetary boundary layer under different weather conditions, and its impact on aerosol concentrations. Particuology, 11(1), pp.34-40, 2013.

Ramanathan, V.C.P.J., Crutzen, P.J., Kiehl, J.T. and Rosenfeld, D., 2001.: Aerosols, climate, and the hydrological cycle. Science, 294(5549), pp.2119-2124., 2001.

Ricchiazzi, P., Yang, S., Gautier, C., and Sowle, D., 1998.: SBDART: A research and teaching software tool for planeparallel radiative transfer in the Earth's atmosphere, B. Am. Meteorol. Soc., 79, 2101–2114, https://doi.org/10.1175/1520-0477(1998)079<2101:SARATS>2.0.CO;2., 1998.

Rienecker, M.M., Suarez, M.J., Gelaro, R., Todling, R., Bacmeister, J., Liu, E., Bosilovich, M.G., Schubert, S.D., Takacs, L., Kim, G.K. and Bloom, S., 2011.: MERRA: NASA's modern-era retrospective analysis for research and applications. Journal of climate, 24(14), pp.3624-3648, 2011.

Sawyer, V., and Li, Z., 2013.: Detection, variations and intercomparison of the planetary boundary layer depth from radiosonde, lidar, and infrared spectrometer, Atmos. Environ., 79, 518-528., 2013.

Smirnov, A., Holben, B.N., Eck, T.F., Dubovik, O. and Slutsker, I., 2000.: Cloud-screening and quality control algorithms for the AERONET database. Remote sensing of environment, 73(3), pp.337-349, 2000.

Stull, R. B.: The energetics of entrainment across a density interface. J. Atmos. Sci., 33, 1260–1267, doi: 10.1175/1520-0469(1976)033<1260:TEOEAD>2.0.CO;2, 1976.

Su, T., Li, J., Li, C., Xiang, P., Lau, A.K.H., Guo, J., Yang, D. and Miao, Y., 2017.: An intercomparison of long-term planetary boundary layer heights retrieved from CALIPSO, ground-based lidar, and radiosonde measurements over Hong Kong. J. Geophys. Res. Atmos., 122(7), 3929- 3943., 2017a.

Su, T., Li, J., Li, C., Lau, A.K.H., Yang, D. and Shen, C.: An intercomparison of AOD-converted PM2. 5 concentrations using different approaches for estimating aerosol vertical distribution. Atmospheric environment, 166, pp.531-542, 2017b.

Su, T., Li, Z. and Kahn, R., 2018.: Relationships between the planetary boundary layer height and surface pollutants derived from lidar observations over China: regional pattern and influencing factors. Atmospheric Chemistry and Physics, 18(21), pp.15921-15935., 2018.

Stull, R. B.: An Introduction to Boundary Layer Meteorology. Kluwer, 670-680 pp, 1988.

Su, T., Li, Z., and Kahn, R., 2019.: A new method to retrieve the diurnal variability of planetary boundary layer height from lidar under different thermodynamic stability conditions. Remote Sensing of Environment., in review., 237, p.111519, 2020.

Formatted: Don't adjust right indent when grid is defined, Don't adjust space between Latin and Asian text, Don't adjust space between Asian text and numbers

Formatted: Font: Not Italic

Tang, G., Zhang, J., Zhu, X., Song, T., Münkel, C., Hu, B., Schäfer, K., Liu, Z., Zhang, J., Wang, L. and Xin, J.~~, 2016.~~: Mixing layer height and its implications for air pollution over Beijing, China. Atmospheric Chemistry and Physics, 16(4), pp.2459-2475~~.~~, 2016.

Wallace, J.M. and Hobbs, P.V.~~, 2006.~~: Atmospheric science: an introductory survey (Vol. 92). Elsevier~~.~~, 2006.

Wang, H., Shi, G.Y., Zhang, X.Y., Gong, S.L., Tan, S.C., Chen, B., Che, H.Z. and Li, T.~~, 2015.~~: Mesoscale modelling study of the interactions between aerosols and PBL meteorology during a haze episode in China Jing–Jin–Ji and its near surrounding region–Part 2: Aerosols' radiative feedback effects. Atmospheric Chemistry and Physics, 15(6), pp.3277-3287~~.~~, 2015.

Wang, H., Li, Z., Lv, Y., Xu, H., Li, K., Li, D., Hou, W., Zheng, F., Wei, Y. and Ge, B.: Observational study of aerosol-induced impact on planetary boundary layer based on lidar and sunphotometer in Beijing. Environmental Pollution, 252, pp.897-906, 2019.

Wang, J., Wang, S., Jiang, J., Ding, A., Zheng, M., Zhao, B., Wong, D.C., Zhou, W., Zheng, G., Wang, L. and Pleim, J.E.~~, 2014.~~: Impact of aerosol–meteorology interactions on fine particle pollution during China's severe haze episode in January 2013. Environmental Research Letters, 9(9), p.094002, 2014.

Wang, Y., A. Khalizov, M. Levy, R. Zhang~~, 2013.~~: New directions: Light absorbing aerosols and their atmospheric impacts, Atmos. Environ., 81, pp.713-715, 2013.

Wang, Y., Li, Z., Zhang, Y., Du, W., Zhang, F., Tan, H., Xu, H., Fan, T., Jin, X., Fan, X. and Dong, Z.~~, 2018.~~: Characterization of aerosol hygroscopicity, mixing state, and CCN activity at a suburban site in the central North China Plain. Atmospheric Chemistry and Physics, 18(16), pp.11739-11752~~.~~, 2018.

Wang, Z., Huang, X. and Ding, A.~~, 2018.~~: Dome effect of black carbon and its key influencing factors: a one-dimensional modelling study. Atmospheric Chemistry and Physics, 18(4), pp.2821-2834, 2018.

Wei, J., Huang, W., Li, Z., Xue, W., Peng, Y., Sun, L., and Cribb.: M. Estimating 1-km-resolution $PM_{2.5}$ concentrations across China using the space-time random forest approach, Remote Sensing of Environment, 231, 111221. https://doi.org/10.1016/j.rse.2019.111221, 2019a.

Wei, J., Li, Z., Sun, L., Peng, Y., Zhang, Z., Li, Z., Su, T., Feng, L., Cai, Z. and Wu, H.: Evaluation and uncertainty estimate of next-generation geostationary meteorological Himawari-8/AHI aerosol products. Science of The Total Environment, 692, pp.~~1-13~~879-891, 2019b.

Yang, D., Li, C., Lau, A.K.H. and Li, Y.~~, 2013.~~: Long-term measurement of daytime atmospheric mixing layer height over Hong Kong. Journal of Geophysical Research: Atmospheres, 118(5), pp.2422-2433, 2013.

Zhang, W., J. Guo, Y. Miao, H. Liu, Y. Song, Z. Fang, J. He, M. Lou, Y. Yan, Y. Li, and P. Zhai~~, 2018.~~: On the summertime planetary boundary layer with different thermodynamic stability in China: A radiosonde perspective. Journal of Climate, 31(4), pp. 1451 – 1465, 2018.

Zhang, Y., Li, Z., Zhang, Y., Li, D., Qie, L., Che, H. and Xu, H.~~, 2017.~~: Estimation of

aerosol complex refractive indices for both fine and coarse modes simultaneously based on AERONET remote sensing products. Atmospheric Measurement Techniques, 10(9), pp.3203-3213, 2017.

Zhang, Y., Y. Li, J. Guo, Y. Wang, D. Chen, and H. Chen, 2019.: The climatology and trend of black carbon in China from 12-year ground observations. Climate Dynamics, doi:10.1007/s00382-019-04903-0, 2019.

Zhou, M., Zhang, L., Chen, D., Gu, Y., Fu, T.M., Gao, M., Zhao, Y., Lu, X. and Zhao, B., 2018.: The impact of aerosol-radiation interactions on the effectiveness of emission control measures. Environmental Research Letters, 2018.

Zou, J., Sun, J., Ding, A., Wang, M., Guo, W. and Fu, C., 2017.: Observation-based estimation of aerosol-induced reduction of planetary boundary layer height. Advances in Atmospheric Sciences, 34(9), pp.1057-1068., 2017.

Figures

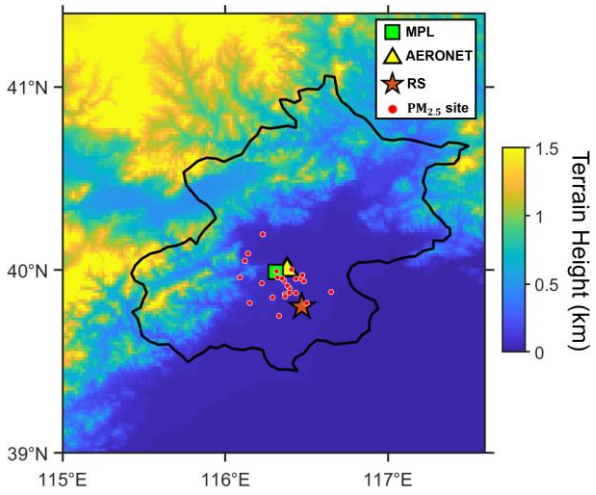

Figure 1. Topography ~~condition~~ of Beijing. The green square indicates the MPL site, and the yellow triangle indicates the AERONET station. The brown star ~~represents~~shows the radiosonde (RS) station, and the red pink dots ~~represent~~show the $PM_{2.5}$ sites.

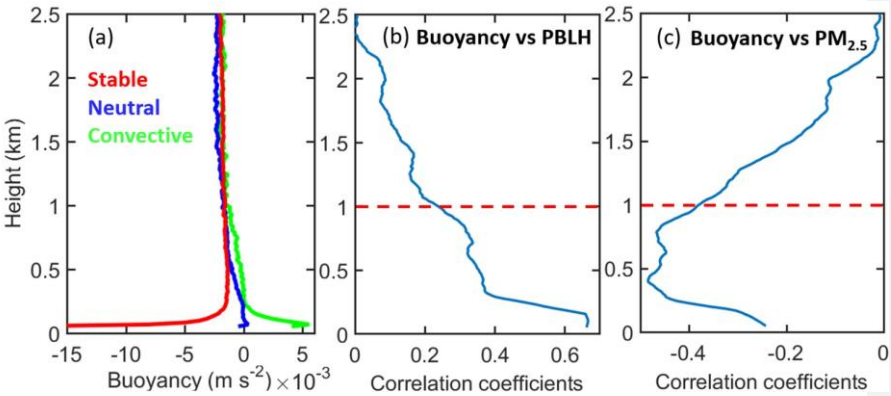

Figure 2. (a) ~~Vertical~~Averaged vertical profiles of buoyancy forcing ~~under~~in stable, neutral, and convective ~~PBL~~PBLs. (b) Height-dependent correlation coefficients between buoyancy and PBLH. (c) Height-dependent correlation coefficients between buoyancy and surface $PM_{2.5}$. ~~Noted~~Note that the PBLH and surface $PM_{2.5}$ are fixed for the entire column, and the buoyancy is height- dependent. The buoyancy ~~within low~~ in the lower atmosphere ~~(~~(< 1 km) ~~exerts~~has the most important impact on the PBLH and surface $PM_{2.5}$. The buoyancy and PBLH are ~~derived~~calculated from RS measurements made at 1400 LT and 2000 LT from 2011 to 2018.

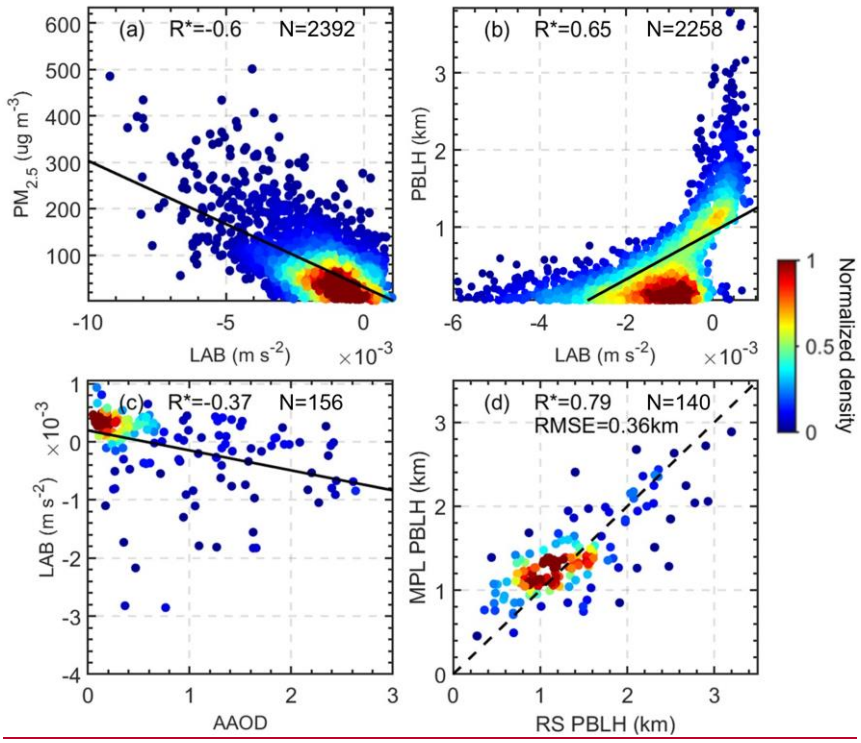

Figure 3. (a) The ~~relationships~~relationship between ~~low~~lower-atmosphere buoyancy (LAB) and $PM_{2.5}$. (b) The ~~relationships~~relationship between LAB and PBLH. (c) The ~~relationships~~relationship between absorbing aerosol optical depth (AAOD) and LAB. In (a, b, c), the LAB and PBLH are derived from RS measurements made at 1400 LT and 2000 LT, and AAOD is derived from AERONET measurements. The black solid lines indicate the best-fit lines from linear ~~regressions~~regression. (d) Comparison of PBLHs derived from the MPL and RS at 1400 LT. ~~Here~~Each panel gives the correlation coefficients (R), sample number (N), and ~~in the following analysis,~~root-mean-square error (RMSE). R with ~~asterisks~~an asterisk indicates that the correlation is statistically

Formatted: Justified

significant at the 99% confidence level. The color-shaded dots indicate the normalized sample density.

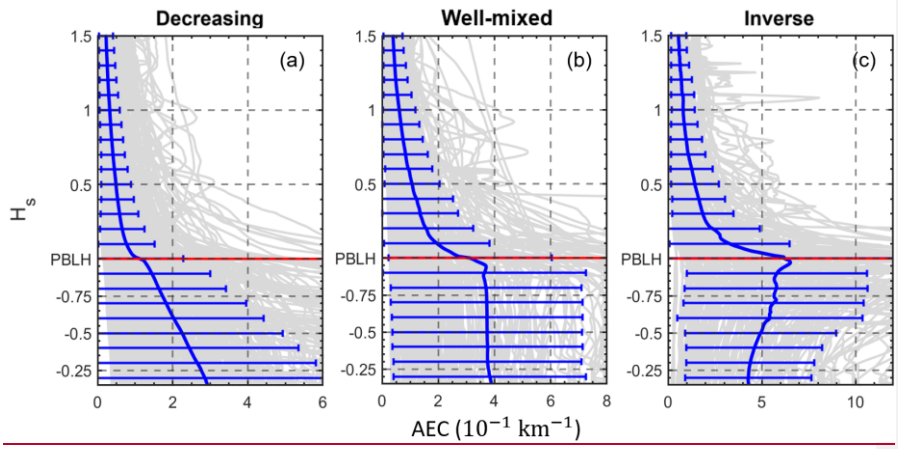

Figure 4. ~~The normalized~~Normalized vertical profiles of aerosol extinction ~~coefficients~~coefficient (AEC) ~~under~~for (a) decreasing, (b) well-mixed, and (c) increasing (i.e., inverse) aerosol structures. ~~The red~~Red line ~~marks~~mark the position of the PBLH, ~~the~~ solid blue lines represent the average ~~profile~~profiles of corresponding profiles, and ~~the~~ error- bars represent the standard deviations.

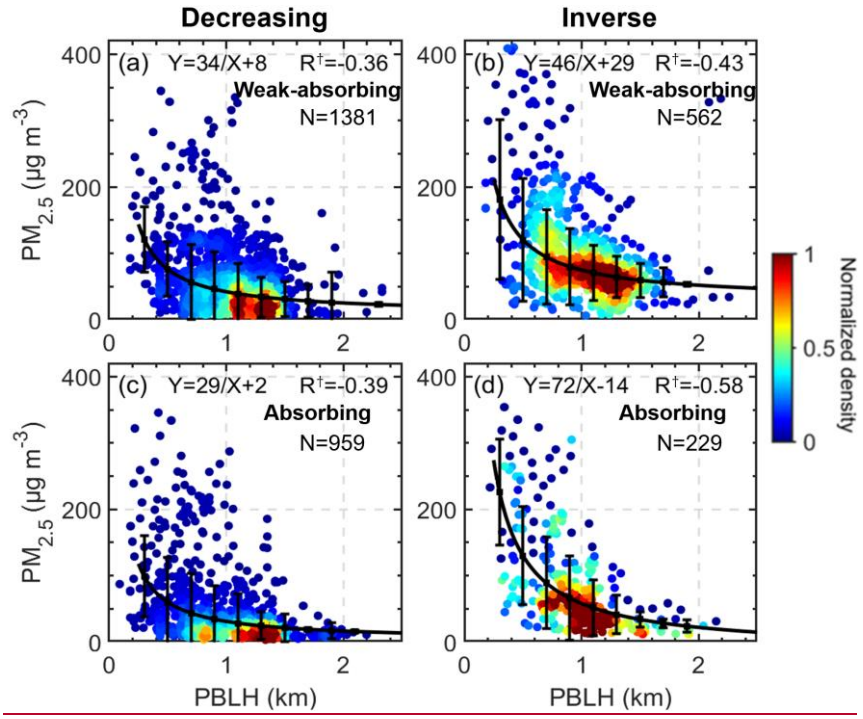

Figure 5. ~~_~~The relationship between MPL-derived PBLH and $PM_{2.5}$ for (a) ~~weak-~~weakly absorbing and (c) absorbing ~~under-~~aerosols for the decreasing ~~aerosols~~aerosol structure. The relationship between MPL-derived PBLH and $PM_{2.5}$ for (b) ~~weak-~~weakly absorbing and (d) absorbing ~~under-inverse-~~aerosols for the increasing (i.e., inverse) aerosol structure. ~~The black~~Black lines represent the inverse ~~fit~~fits, and the whiskers indicate the standard deviations. The~~-detailed~~ fitting functions and number of samples are given ~~at the top of~~in each panel, along with the correlation coefficient ($R^{\dagger}$) for the inverse fit.

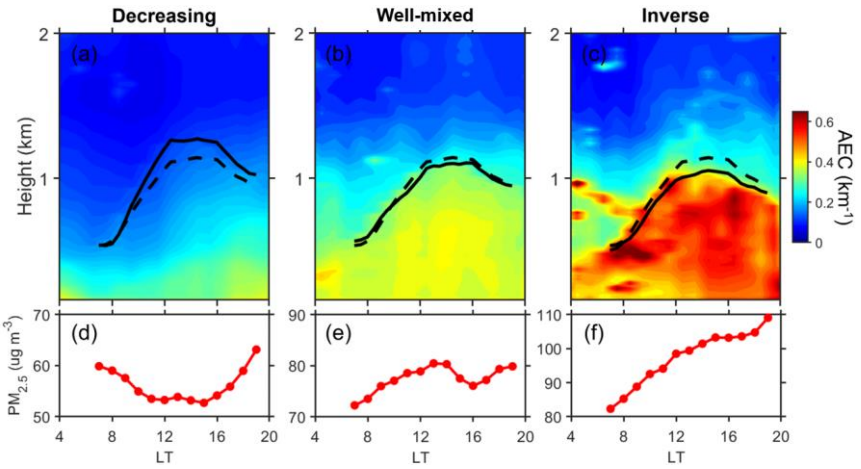

Figure 6. ~~Diurnal~~The averaged diurnal variations in AEC for (a) decreasing, (b) well-mixed, and (c) increasing (i.e., inverse) aerosol structures. ~~The solid~~Solid black lines indicate the ~~corresponding PBLH~~ averaged diurnal cycles~~. The dashed black line represents~~ of MPL-derived PBLH under the different aerosol structures. Dashed black lines represent the mean MPL-derived PBLH diurnal ~~cycle~~cycles. (d, e, f) The ~~corresponding~~averaged diurnal variations in surface $PM_{2.5}$ under the different aerosol structures.

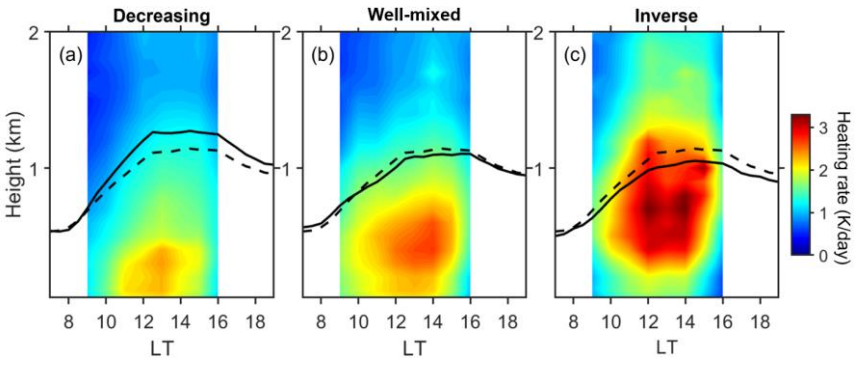

Figure 7. The ~~profiles of~~ averaged diurnal variations in aerosol radiative forcing in the vertical for (a) decreasing, (b) well-mixed, and (c) increasing (i.e., inverse) structures of aerosol loading. ~~The solid~~Solid black lines indicate the ~~corresponding PBLH~~ mean diurnal cycles~~. The dashed~~ of MPL-derived PBLH under different aerosol structures. Dashed black ~~line represents~~lines represent the mean MPL-derived PBLH diurnal ~~cycle~~cycles.

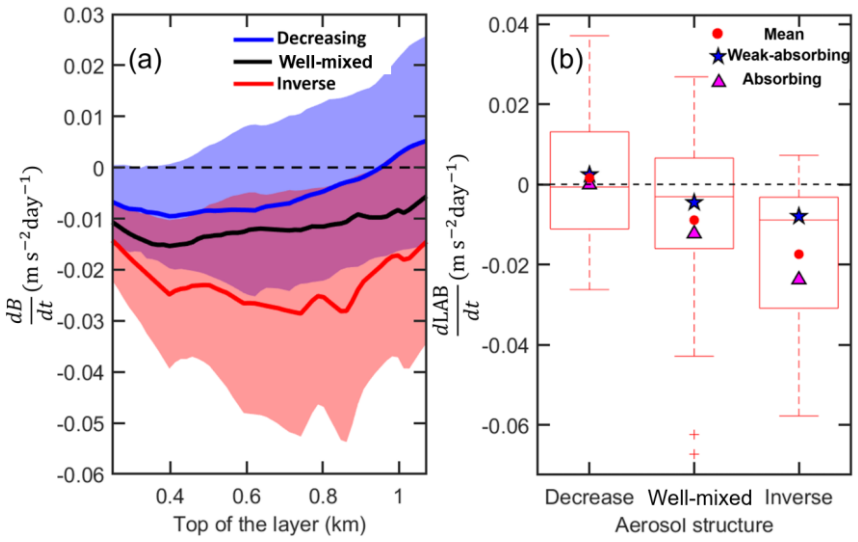

Figure 8. (a) The rate of change ~~rate~~ in buoyancy (dB/dt) in a ~~certain~~ layer of the lowest atmosphere ~~under~~for decreasing (blue), well-mixed (black), and inverse (red) aerosol structures during noontime. The bottom of the layer is the surface, and the rate of change in buoyancy is subjected to the top of the layer. The shaded areas show the standard ~~deviation~~ deviations of the rate of change ~~rate~~ in buoyancy. (b) Box-and-whisker plots showing 10th, 25th, 50th, 75th, and 90th percentile values of the rate of change ~~rate~~ in LAB (buoyancy within lowest ~~1km~~1 km) during noontime. ~~The red~~Red dots indicate the mean values, ~~while the~~and blue stars and pink triangles show the means for ~~weak~~ weakly absorbing (SSA > 0.9) and absorbing (SSA < 0.85) cases.

Formatted: Font color: Red

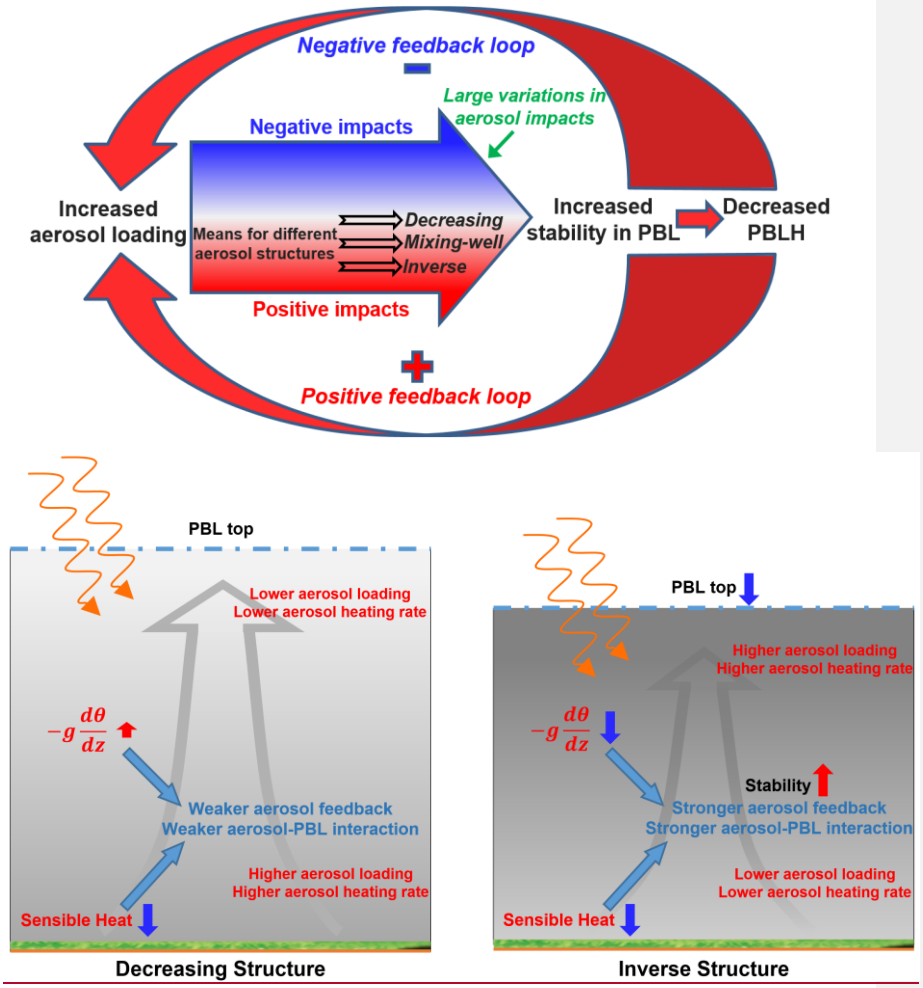

Figure 9. Schematic ~~diagram showing the~~ diagrams describing aerosol-PBL interactions ~~between aerosols, stability,~~when decreasing and ~~the PBL that comprise positive impacts (red arrows) and negative impacts (blue arrows). The aerosol impacts on stability largely vary with meteorology and aerosol conditions, and the means of aerosol impacts on stability for different~~inverse aerosol structures are ~~indicated in~~present. The blue dash-dotted line indicates the top of the PBL. Orange curved arrows indicate solar radiation. The background grey arrow sketches the vertical transport of

834 humidity, aerosols, and heat. The background greyscale indicates the ~~diagram~~pollution

835 level.

836

837

838

839

840

841

842

Formatted: Font color: Auto